1-1-2014

Photodetachment cross sections of the C2nH- (n=1-3) hydrocarbon-chain anions

Nicolas Douguet

Viatcheslav Kokoouline
University of Central Florida

Ann E. Orel

Photodetachment cross sections of the $C_{2n}H^-$ ($n = 1$–3) hydrocarbon-chain anions

Nicolas Douguet,[1] Viatcheslav Kokoouline,[2] and Ann E. Orel[1]
[1]*Department of Chemical Engineering and Materials Science, University of California, Davis, California 95616, USA*
[2]*Department of Physics, University of Central Florida, Orlando, Florida 32816, USA*
(Received 23 September 2014; published 2 December 2014)

We report theoretical results of the low-energy photodetachment cross sections of the C_2H^-, C_4H^-, and C_6H^- hydrocarbon-chain anions. The complex Kohn variational technique is used to calculate molecular-frame transition dipole moments from the anion ground state to a photoelectron in the continuum of the neutral radical. We employ the Franck-Condon approximation and include interchannel electronic coupling to determine the low-energy photodetachment cross sections and asymmetry parameters. We discuss the behavior of the cross section, especially near thresholds, and describe the role of electronic resonances and excited channels. The theoretical results reproduce the main characteristics of recent measurements of absolute photodetachment cross sections.

DOI: 10.1103/PhysRevA.90.063410 PACS number(s): 33.80.Eh, 98.38.Dq, 95.30.Ft

I. INTRODUCTION

During the last decade, numerous astrophysical observations [1–7] have confirmed the long-standing prediction by Herbst [8] on the existence of negatively charged ions in the interstellar medium (ISM). These recent discoveries have triggered a revived interest in understanding the general formation and destruction mechanisms of these exotic species [9–14]. The main destruction pathways of anions in astronomical objects exposed to ultraviolet radiations is the detachment of a bound electron following the absorption of a photon with energy $\hbar\omega > EA$, where EA is the electron affinity of the A radical,

$$A^- + \hbar\omega \rightarrow A + e^-. \tag{1}$$

Numerous laboratory studies have investigated the photodetachment of various carbon chain anions. Pinot *et al.* [15] measured the electronic spectra of the ions $C_{2n}H^-$ ($n = 2$–4) near their lowest detachment thresholds. They reported sharp transitions although no excited valence states exist for the ions and observed the signature of excited dipole bound states. More recently, Best *et al.* [9] have used a new developed method to measure the absolute photodetachment cross section of the hydrocarbon-chain anions $C_{2n}H^-$ ($n = 1$–3), to a precision better than 25%. Their cross sections were obtained only at a few photon energies, within approximately 1 eV, but nonetheless allowed a qualitative comparison with the empirical scaling law of Millar *et al.* [16]. According to the latter model, the behavior of the photodetachment cross section σ, as a function of the photon energy $\epsilon_p = \hbar\omega$, follows the empirical formula,

$$\sigma(\epsilon_p) = \sigma_\infty \sqrt{1 - \frac{EA}{\epsilon_p}}. \tag{2}$$

The quantity σ_∞ can be extracted from the experimental data and be further used in the astrophysical models. The use of formula (2) to fit the experimental data [9] seems to work relatively well for both C_2H^- and C_6H^- ions, although it fails to reproduce the correct detachment threshold energy of C_2H^-. On the other hand, the measured cross section of C_4H^- far above threshold disagrees by a factor of four with the scaling formula obtained by extracting the coefficient σ_∞ from the near-threshold part of the cross section. Using the same experimental method, Kumar *et al.* [12] measured the photodetachment cross section for both CN^- and C_3N^- ions. They observed significantly larger values for the photodetachment cross sections of these species in comparison with the hydrocarbon-chain ions and discuss the astrophysical consequences. Note that the latter cross sections were only measured at a single laser frequency, such that comparison with the model of Millar *et al.* [16] could not be addressed. However, the value of the constant σ_∞ could still be extracted from the known affinities of the radicals, assuming that the photon energy does not correspond to the position of a resonance.

There are several motivations for studying the photodetachment process of these molecular anions from a theoretical standpoint. First, the number of energy points in the measured photodetachment cross section is insufficient to enable a rigorous comparison with the astrophysical model. The principal advantage of a first-principles calculation that reproduces quantitatively the measured cross sections is to check the validity of the empirical formula (2) and the overall behavior of the cross section. Secondly, the model of Millar *et al.* does not consider the role of electronic resonances and excited target states in the photodetachment process. In fact, the associated radicals of the three studied ions possess a low-lying excited electronic state, which becomes an open channel at large enough photon energy. The existence of such channels can modify the overall shape of the photodetachment cross section and their role is explicitly taken into account in our calculations.

The electron spectrum in the photodetachment cross sections of the small anion C_2H^- has been extensively studied in past experimental works [17–19] and shows a complex structure indicating strong vibronic couplings due to the presence of a low-energy conical intersection. The spectrum exhibits a complex photoelectron angular distribution, characterized by an asymmetry parameter strongly dependent on the particular absorption peaks. The same characteristics have also been observed for the larger anions [15]. The complete study of the photoelectron experimental spectra of Ref. [18] lies out of the scope of the present work, which is restricted to the Franck-Condon (FC) approximation and does not account

for detailed features of the photodetachment process due to the strong vibronic couplings involved in vibrationally excited states. The scattering calculations are performed at fixed nuclei, which within the FC approximation could be applied to any vibrational state if the appropriate vibrational overlap integrals were computed exactly. Here, we restrict the calculations to transitions to the ground vibrational state of electronically open channels, which should represent the major contribution in the photodetachment cross section. Therefore, there exists in the present approach a direct correspondence between the photon energy and the photoelectron energy associated with each electronically open channel.

On the other hand, our study attempts to reproduce quantitatively the vibrationally unresolved photodetachment cross section for large carbon chain anions and answer some of the open questions arising from the experimental measurements. The values of the molecular-frame (MF) transition dipole moments computed in the present work and the determination of the asymmetry parameter as a function of the photoelectron energy could serve as useful information for a deeper analysis of the spectrum.

In the next section, we briefly describe the important aspects of the photodetachment process and present our theoretical approach based on the complex Kohn variational method. The results for the photodetachment cross sections of the C_2H^-, C_4H^-, and C_6H^- anions are presented in Sec. III. Finally, Sec. IV is devoted to our conclusions.

II. THEORETICAL APPROACH TO PHOTODETACHMENT

Early works on photodetachment focused on the description of the near-threshold energy dependence of the cross section. In his 1948 seminal paper, Wigner [20] demonstrated that the threshold dependence of the collision cross section of two product particles depends solely on their long-range interaction potential. For the photodetachment process, assuming that the interaction potential falls off faster than r^{-2} (thus neglecting dipole interactions), Wigner derived that the cross section for l-wave photoelectron scattering is given by $\sigma(\epsilon_e) \propto {\epsilon_e}^{l+\frac{1}{2}}$, where $\epsilon_e = \epsilon_p - EA$ is the asymptotic electron energy. At this point, it is instructive to note that Eq. (2) at energies just above threshold ($\epsilon_p - EA \ll 1$) takes the form $\sigma(\epsilon_p) \propto \sqrt{\epsilon_p - EA}$ and thus converges to the Wigner threshold law for s-wave scattering.

The result of Wigner can be generalized presupposing that the potential interaction is of finite range and one can expand the cross section in a Taylor series,

$$\sigma(\epsilon_e) = {\epsilon_e}^{l_o+\frac{1}{2}}(a_0 + a_1\epsilon_e + a_2\epsilon_e^2 + \cdots), \tag{3}$$

where l_o represents the lowest symmetry allowed electron angular momentum. O'Malley [21] considered the effect of the long-range dipole and quadrupole potentials on the photodetachment cross section near threshold and showed how the power series expansion in Eq. (3) is accordingly modified. Reed *et al.* [22] used group theory to derive the general limiting behavior of the cross section for polyatomic ions. Using the Born-Oppenheimer approximation and partial orthogonalization of the plane wave to the highest occupied orbital, they compute the cross sections for the H^-, OH^-, O_2^-, N_2H^-, and $C_5H_5^-$ ions. Despite the set of approximations, which were employed, Reed *et al.* [22] obtained relative cross sections that agree well with experimental measurements up to 1 eV above threshold.

The complex Kohn variational method has been used extensively in electron scattering by neutral or ionic targets. Because the method does not rely on a single-center expansion of the electron-target interaction, it is well adapted to the case of polyatomic systems. The transition dipole moments obtained from the Kohn trial function have been shown to be variationally stable [23] and the method has been applied in past studies on the photoionization of diatomic molecules such as H_2 and CO [24,25]. The Kohn technique was also used to calculate the radiative electron attachment to the CN radical [13] and to study the photodetachment of $HOCO^-$ [26].

The technical details of the complex Kohn variational method have been extensively addressed elsewhere [27–30] and the implementation of the Kohn principle in calculations of photoionization cross sections and photoelectron angular distributions has already been presented in several studies [13,31–33]. For these reasons, we only summarize the main aspects of the method here.

In the Kohn method, the electron-neutral scattering wave function, with the neutral molecule in a state Γ_o, is expressed as

$$\Psi^-_{\Gamma_o l_o m_o} = \sum_\Gamma \hat{A}\left(\chi_\Gamma F^-_{\Gamma\Gamma_o}\right) + \sum_i d_i^{\Gamma_o}\Theta_i, \tag{4}$$

where the first sum runs over energetically open neutral states described by $N-1$ electron wave functions χ_Γ and the second sum runs over N electron configuration-state functions Θ_i representing penetration terms. The operator $\hat{A}$ ensures the antisymmetrization between the continuum and neutral wave functions. The continuum functions $F^-_{\Gamma\Gamma_o}$ are expanded in the following way:

$$F^-_{\Gamma\Gamma_o}(\mathbf{r}) = \sum_i c_i^{\Gamma\Gamma_o}\phi_i(\mathbf{r}) + \sum_{lm}\big[f_l(k_\Gamma r)\delta_{ll_o}\delta_{mm_o}\delta_{\Gamma\Gamma_o} + T^{\Gamma\Gamma_o}_{ll_omm_o}h_l^-(k_\Gamma r)\big]Y_{lm}(\hat{\mathbf{r}})/r, \tag{5}$$

where f_l and h_l^- are partial-wave continuum radial functions behaving asymptotically as regular and incoming Riccati-Bessel functions and ϕ_i is a set of square integrable functions. Using the variational method, a set of linear equations for the coefficients $c_i^{\Gamma\Gamma_o}$, $d_i^{\Gamma_o}$, and $T^{\Gamma\Gamma_o}_{ll_omm_o}$ is obtained and its solution leads to the optimized results.

The photoionization cross section is determined from the following matrix elements expressed in terms of body-frame amplitudes calculated at the equilibrium geometry $\mathcal{Q}_o$ of the anion:

$$I^\mu_{\Gamma_o}(\mathcal{Q}_o) = \langle\Psi_o|r^\mu\big|\Psi^-_{\Gamma_o l_o m_o}\rangle. \tag{6}$$

The function Ψ_o represents the initial electronic state of the target molecule and r^μ is the dipole operator defined in the length form as

$$r^\mu = \begin{cases} z, & \mu = 0 \\ \mp(x \pm iy)/\sqrt{2}, & \mu = \pm 1. \end{cases} \tag{7}$$

To obtain an amplitude representing an ejected electron with momentum $\boldsymbol{k}_{\Gamma_o}$ associated with a particular neutral channel

and direction of light polarization $\hat{\epsilon}$, the matrix element in Eq. (6) must be combined in a partial wave series,

$$I_{\hat{k}_{\Gamma_o},\hat{\epsilon}}(\mathcal{Q}_o) = \sqrt{\frac{4\pi}{3}} \sum_{l_o m_o \mu} i^{l_o} e^{-i\delta_{l_o}} I^{\mu}_{\Gamma_o} Y^*_{1\mu}(\hat{\epsilon}) Y^*_{l_o m_o}\left(\hat{k}_{\Gamma_o}\right). \quad (8)$$

The doubly differential partial cross section for formation of the ground vibrational state in the Γ_o electronic state, and relative to the fixed-body frame of the molecule, is given in the FC approximation by

$$\frac{d^2\sigma^{\Gamma_o}}{d\Omega_{\hat{k}} d\Omega_{\hat{\epsilon}}} = \frac{8\pi\omega}{3c} \left|S^{\Gamma_o}_{v_o^-,v_o}\right|^2 \left|I_{\hat{k}_{\Gamma_o},\hat{\epsilon}}(\mathcal{Q}_o)\right|^2. \quad (9)$$

In the above expression, c is the speed of light, ω represents the photon energy, and $S^{\Gamma_o}_{v_o^-,v_o} = \langle \zeta^-_{v_o} | \zeta^{\Gamma_o}_{v_o} \rangle$ is the vibrational overlap between the ground vibrational state $|\zeta^-_{v_o}\rangle$ of the anion and the ground vibrational state $|\zeta^{\Gamma_o}_{v_o}\rangle$ of the product radical in the Γ_o electronic state. To compute a laboratory-frame photoelectron angular distribution, Eq. (9) is averaged over all orientations of the target anion. The resulting differential cross section takes the form,

$$\frac{d\sigma^{\Gamma_o}}{d\Omega} = \left\langle \frac{d^2\sigma^{\Gamma_o}}{d\Omega_{\hat{k}} d\Omega_{\hat{\epsilon}}} \right\rangle_{\text{av}} = \frac{\sigma^{\Gamma_o}}{4\pi} [1 + \beta^{\Gamma_o} P_2(\cos\theta)], \quad (10)$$

where P_2 is the Legendre polynomial of order 2, θ is the angle between the light polarization direction $\hat{\epsilon}$, and the photoelectron momentum direction $\boldsymbol{k}_{\Gamma_o}$, and β^{Γ_o} is the asymmetry parameter. The partial cross section σ^{Γ_o} is obtained by averaging over the polarization directions and integrating over photoelectron directions:

$$\sigma^{\Gamma_o} = \frac{8\pi\omega}{3c} \left|S^{\Gamma_o}_{v_o^-,v_o}\right|^2 \sum_{l_o m_o \mu} \left|I^{\mu}_{\Gamma_o}(\mathcal{Q}_o)\right|^2. \quad (11)$$

The vibrational overlap can in principle be computed exactly in the multidimensional space spanned by the degrees of freedom of the molecule. However, for the large chain ions it leads to very demanding and unneeded computational work. This approach can be greatly simplified because the harmonic frequencies and normal coordinates of the anion and radical lowest states happen to be very similar. In the approximation of equal normal coordinates and frequencies for the anion and radical states, the nuclear coordinate shift between the minima of these potentials becomes the fundamental quantity that determines the vibrational overlap in the harmonic approximation. For the photodetachment from the vibrational ground state, the overlap will be represented by a simple product of Gaussian integrals corresponding to each dimensionless stretching coordinate Q_i ($i = 1, \ldots, N$). Choosing $\mathcal{Q}_o$ as the origin of the reference system ($\mathcal{Q}_o = 0$), and considering that the anion and radical minima are displaced along each mode by a quantity Δ_i, the total overlap can be readily written as

$$\begin{aligned} S^{\Gamma_o}_{v_o^-,v_o} &= \left(\frac{1}{\pi}\right)^{\frac{N}{2}} \prod_{i=1}^{N} \int_{-\infty}^{\infty} e^{-\frac{Q_i^2}{2}} e^{-\frac{(Q_i+\Delta_i)^2}{2}} dQ_i, \\ &= \left(\frac{1}{\pi}\right)^{\frac{N}{2}} \prod_{i=1}^{N} e^{-\frac{\Delta_i^2}{4}} \int_{-\infty}^{\infty} e^{-z^2} dz. \end{aligned} \quad (12)$$

Using the value of the standard integral and introducing the total displacement $\Delta = \sqrt{\Delta_1^2 + \Delta_2^2 + \cdots + \Delta_N^2}$ between both electronic potential minimum in the metric of the dimensionless normal coordinates space, we obtain the simple formula,

$$S^{\Gamma_o}_{v_o^-,v_o} = e^{-\frac{\Delta^2}{4}}. \quad (13)$$

The values of the vibrational overlap is used to calculate the partial cross section (11) related to each open channel Γ_o. The total cross section is then obtained by summing the contribution from all open channels.

III. RESULTS

A. Photodetachment of C_2H^-

The photodetachment of C_2H^- has been thoroughly investigated from an experimental standpoint [9,17–19]. The main configuration of the electronic ground state $\widetilde{X}\,^1\Sigma^+$ of C_2H^- is $(\ldots 4\sigma^2 1\pi^4 5\sigma^2)$ and its photodetachment to the lowest $\widetilde{X}\,^2\Sigma^+$ state of C_2H is characterized by the removal of an electron from the HOMO and requires 2.969 eV [17,19] of energy. At about 0.46 eV above the lowest detachment threshold, an electron can also detach from one of the degenerate π orbitals to form the $\widetilde{A}\,^2\Pi$ excited state of C_2H.

In the electron-molecule scattering calculations, the neutral and anion electronic states are described with the aug-cc-pVTZ basis set and through a complete active space configuration interaction (CAS-CI) calculation, which includes 10 molecular orbitals (MOs) with frozen carbon core orbitals. In order to get a consistent description of the photodetachment process, one should accurately represent the initial state of C_2H^- as well as the electron scattering from both target channel states. For this reason, the MOs are optimized by averaging the natural orbitals (NOs) of the $\widetilde{X}\,^1\Sigma^+$, $\widetilde{X}\,^2\Sigma^+$, and $\widetilde{A}\,^2\Pi$ states in order to reproduce the important characteristics of each state and to obtain reasonable values of the excitation and detachment energies. The computed dipole moment of C_2H in its ground state is rather small, 0.74 D, in good agreement with reported values in the literature [10,34], whereas the dipole moment of the excited $^2\Pi$ state is relatively large, 3.15 D. The obtained value for the affinity of C_2H is 2.17 eV and its excitation energy to the $^2\Pi$ state is calculated to be 0.56 eV. The latter values are in relatively good agreement with the experimental measurements. Let us emphasize that the difficulty in obtaining high precision values of all parameters comes from our unified description of different states, which can also have a different number of electrons. Because the method requires a single active space of MOs, it can lead to difficulties in treating the N and $N+1$ electron systems in a balanced fashion. This problem is partly overcome by our choice of a large CAS and by using averaged optimized orbitals for the anion and radical states. In addition, we have verified that, as long as our calculated affinity is in reasonable agreement with the experimental value, the photodetachment cross section is not very sensitive to further improvements.

Potential energy curves, calculated at a higher level of structure calculations by including all double excitations outside the CAS, are shown in Fig. 1 as a function of the R_{CC} bond distance. The conical intersection, located at about

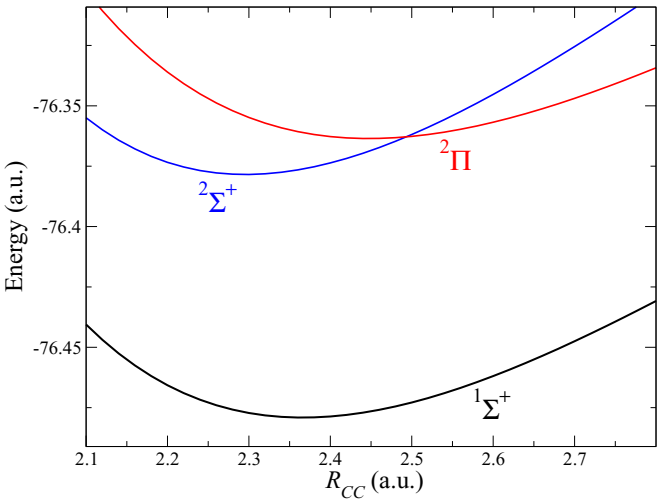

FIG. 1. (Color online) Potential energy curves in atomic units (a.u.), as a function of the R_{CC} distance, for the $^2\Sigma^+$ and $^2\Pi$ states of C_2H, and the $^1\Sigma^+$ ground state of C_2H^-. The R_{CH} distance is fixed at 2.00 a.u.

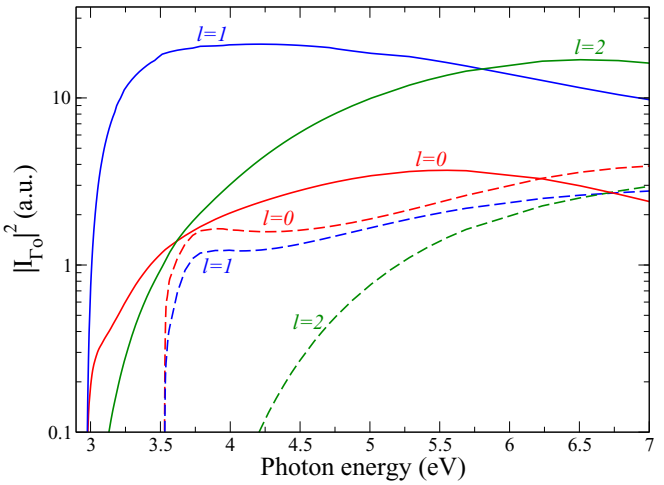

FIG. 2. (Color online) Square of the transition dipole moments of C_6H^- for the s, p, and d partial wave contributions associated with the $^2\Sigma^+$ (solid lines) and $^2\Pi$ (dashed lines) channels of C_2H as a function of the photon energy.

2.50 a.u., is responsible for strong vibronic couplings between excited vibrational states. Note that the equilibrium bond distance for the neutral $^2\Sigma^+$ and $^2\Pi$ states, respectively, at 2.30 and 2.45 a.u., are significantly shifted from the equilibrium position, at 2.365 a.u., of the $^1\Sigma^+$ ground state of C_2H^-. Hence, the FC factors for both electronic states are expected to be somehow smaller than unity. Both potential energy curves of the C_2H lowest states agree well with past calculations by Peric *et al.* [35]. Finally, at this level of calculation, we obtain an improved vertical affinity of 2.80 eV.

In the Kohn calculation, we have included angular momenta up to $l = 5$ and considered scattering in total Σ and Π symmetries (electron+radical), since they are (in the dipole approximation) the only symmetries involved in the photodetachment of the C_2H^- electronic ground state. The transition dipole moments squared of the lowest electronic angular momenta are displayed for each channel in Fig. 2 as a function of the photon energy. The detachment threshold energy is taken at the experimental value of 2.969 eV. One observes that p-wave detachment largely dominates for photodetachment to the $^2\Sigma^+$ radical state, while the s-wave transition dipole moment dominates the overall contribution from p waves in the photodetachment to the excited radical state. The form of the s and p partial waves transition dipole moments depicts an oscillating behavior (better visualized on a linear scale) just above the $^2\Pi$ channel threshold, which is caused by the supercritical value of the dipole moment in that channel [21]. A detailed discussion on this particular threshold dependence of the cross section is given for the case of C_4H^- in Sec. III B. Finally, note that the calculated dominant p- and s-wave emission, respectively, in the photodetachment to the $^2\Sigma^+$ and $^2\Pi$ states, agrees with the experimental findings [17–19].

Experimentally, the asymmetry parameter β^{Γ_o} in Eq. (10) is the relevant measurable quantity, which gives information on the photodetachment angular distribution. The calculated values of the asymmetry parameters for both channels are displayed in Fig. 3, as a function of the photoelectron energy relative to each channel threshold. Bearing in mind that $-1 \leqslant \beta \leqslant 2, \beta = 0$ for s wave, $\beta = 2$ for p wave, and $\beta = -1$ for $(s + d)$ wave, the overall behavior of the asymmetry parameters can easily be interpreted. The asymmetry parameter β^{Σ} rises sharply from near zero values with the photoelectron energy because the contribution from p waves becomes rapidly dominant. Then, β^{Σ} starts to drop smoothly with energy as the p-wave contribution decreases and the d-wave contribution increases. Ervin and Lineberger [17] reported values of the asymmetry parameter between 1.4 and 1.6 for allowed (in the FC approximation) photodetachment transitions to the $\widetilde{X}\,^2\Sigma^+$ state at a photon energy of 3.531 eV (0.562-eV photoelectron energy), while Zhou and co-workers [19] measured $\beta = 1.9$ at a photon energy of 3.494 eV (0.525-eV photoelectron energy).

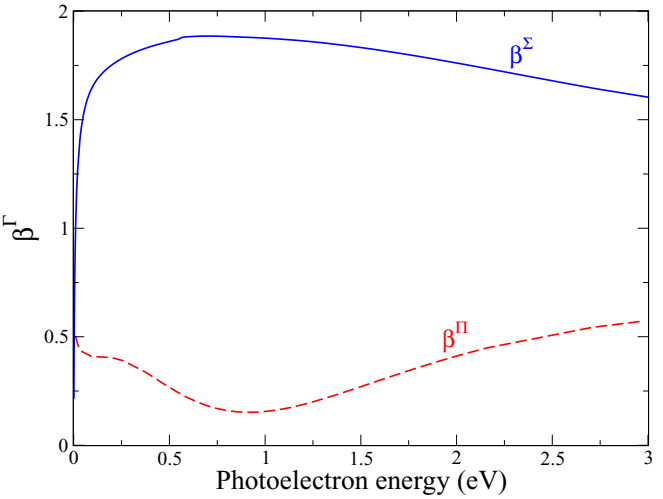

FIG. 3. (Color online) Asymmetry parameters β^{Σ} and β^{Π} for C_2H^- photodetachment as a function of the photoelectron energy relative to each channel threshold.

Our calculated value $\beta = 1.8$ in that energy range is seen to agree well with the reported value by Zhou *et al.* [19].

By using a higher laser frequency of 4.657 eV (1.688-eV photoelectron energy), Taylor *et al.* [18] measured the asymmetry parameter to be 1.04 ± 0.25 for photodetachment to the ground vibrational state $\widetilde{X}\,^2\Sigma^+(00^00)$ of C_2H. Our calculated asymmetry parameter at the latter photon energy is seen to overestimate the experimental measurement. However, we note that the experimental value of the asymmetry parameter for photodetachment of the C_2D^- isotope [18] at the same photon energy is as high as $\beta = 1.51$. This fact probably indicates a strong geometry dependence of the asymmetry parameter, which is not accounted for in our Franck-Condon calculations. The β^Π asymmetry parameter clearly shows a specific threshold behavior as it keeps a constant value $\sim$0.5 at low photoelectron energy and varies only slowly as a function of the electron energy. Zhou and co-workers [19] reported a value of $\beta = -0.3$ for the emission peak to the $\widetilde{A}\,^2\Pi(00^00)$ state. Comparison with our results in this case is complicated by the particularly severe breakdown of the Born-Oppenheimer approximation in C_2H near the $^2\Pi$ channel opening due to the presence of the conical intersection (see Fig. 1). Thus, strong vibronic interactions are expected in the form of Renner-Teller coupling within the $\widetilde{A}\,^2\Pi$ state and Herzberg-Teller coupling between the $\widetilde{X}\,^2\Sigma^+$ and $\widetilde{A}\,^2\Pi$ states and our fixed nuclei calculations should not describe accurately such transitions. On the other hand, Taylor *et al.* [18] measured $\beta \cong -1$ for the peak corresponding to the $\widetilde{A}\,^2\Pi(01^-0)$ state and this state is not coupled to the $\widetilde{X}\,^2\Sigma^+$ because it has overall Σ^- symmetry. In this case, the calculated asymmetry parameter for the $^2\Pi$ channel seems to be too large and should drop rapidly towards negative value. A possible explanation for this disagreement is that bending of the molecule and inclusion of the Renner-Teller effect could significantly decrease the asymmetry parameter.

The different values of the frequencies and equilibrium bond distances are needed to calculate the FC factors. Because the results of different *ab initio* calculations and experimental measurements disagree to some extent with each other, we have performed additional calculations using different methods with the MOLPRO suite of codes. The equilibrium and vibrational frequencies of the anion and radical electronic states are listed in Table I. The CAS-CI/I corresponds to the calculation previously described in the text, while CAS-CI/II is a similar calculation performed in a CAS of orbitals optimized on the anion ground state, and obtained through a MCSCF calculation. Despite the fact that the table shows a reasonable agreement between different calculations and the experimental values, discrepancies exist for different characteristics of the states and will ultimately lead to an uncertainty in the values of the FC factors. One important fact demonstrated by the results of Table I is that the frequencies are similar for the different electronic states. Although not shown in the table, the same is also true for the normal coordinates. Thus, we conclude that Eq. (13) should represent a good approximation. Because the CAS-CI/I calculation should be the most consistent between values associated with different states and we have not found experimental equilibrium bond distance values for C_2H^-, we used the CAS-CI/I parameters and the anion frequencies to determine the FC factors. We obtained $|\langle\zeta^-_{v_o}|\zeta^\Sigma_{v_o}\rangle|^2 = 0.83$ and $|\langle\zeta^-_{v_o}|\zeta^\Pi_{v_o}\rangle|^2 = 0.73$, and we estimate the uncertainty in our calculated values to be, respectively, 1% and 10%.

The total cross section is plotted as a function of the photon energy in Fig. 4 and compared with the experimental measurements by Best *et al.* [9] and with the model of Millar *et al.* [16] defined in Eq. (2). Our theoretical cross section agrees relatively well with the experimental values considering the experimental error bars and the uncertainty in our calculation, which we estimate to be similar to the experimental one. The discrepancy of about 25% at 4.03-eV photon energy is not so surprising because the FC approximation should not be very precise in that energy range for reasons discussed above. From the figure, one observes the importance of taking into account the excited $^2\Pi$ channel, which causes the photodetachment cross section to rise faster at large photon

TABLE I. Equilibrium bond distances and vibrational frequencies for the $^2\Sigma^+$ and $^2\Pi$ states of C_2H, and the $^1\Sigma^+$ ground state of C_2H^-. The bond distances are given in atomic units and the frequencies in wave numbers.

Mol.	State	Method	R_{CC}	R_{CH}	ω_3(C-C)	ω_2(bend)	ω_1(C-H)	Taken from
C_2H	$\widetilde{X}\,^2\Sigma^+$	CAS-CI/I	2.301	1.998				This work
		CAS-CI/II	2.291	1.995	2003	302	3521	This work
		UCCSD	2.281	2.003	2061	370	3489	This work
		EOMIP	2.270	1.995	2109	512	3521	Ref. [36]
		CIPSI	2.312	2.032	1975	570	3346	Ref. [37]
		Expt.	2.300	1.968	1848	389	3612	Ref. [38]
C_2H	$\widetilde{A}\,^2\Pi$	CAS-CI/I	2.451	2.011				This work
		CAS-CI/II	2.441	2.013	1621	441	3436	This work
		EOMIP	2.411	2.009	1795	571	3424	Ref. [36]
		CIPSI	2.461	2.009				Ref. [37]
		Expt.	2.434	2.003				Ref. [38]
C_2H^-	$\widetilde{X}\,^1\Sigma^+$	CAS-CI/I	2.364	2.010				This work
		CAS-CI/II	2.367	2.009	1766	436	3413	This work
		CCSD	2.367	2.018	1813	447	3367	This work
		Expt.			1800	505		Ref. [17]

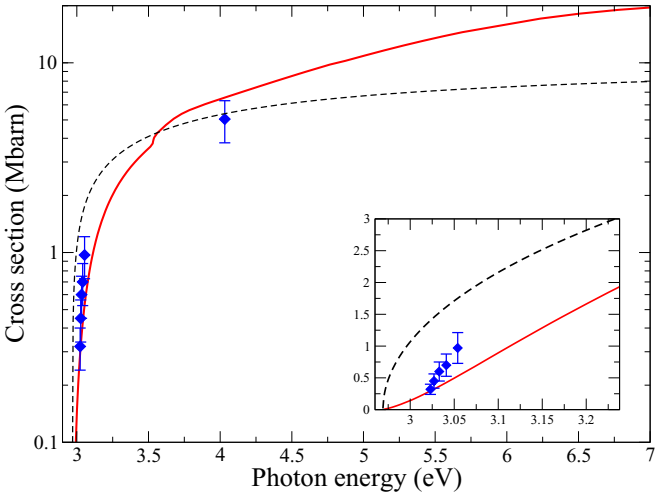

FIG. 4. (Color online) Calculated total cross section (solid line) in C_2H^- photodetachment as a function of the photon energy. The dashed line represents the model defined in Eq. (2) with the known electron affinity as threshold energy. Experimental points are taken from Ref. [9] with associated 25% error bars. The inset on the bottom right shows the near threshold part of the cross section.

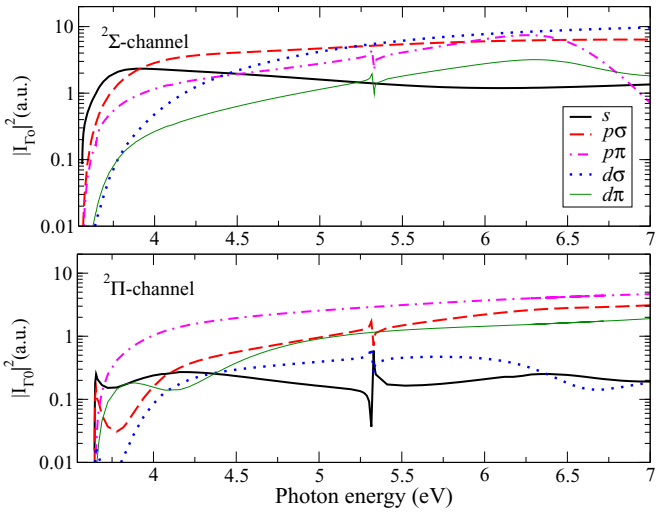

FIG. 5. (Color online) Square of the transition dipole moments of C_4H^- for different partial waves associated with the $^2\Sigma^+$ (upper panel) and $^2\Pi$ (lower panel) channels as a function of the photon energy.

energy. At energy just above the lowest detachment threshold, our calculation seems to reproduce the general trend in the behavior of the experimental data. In Ref. [9], the low-energy part of the cross section was fitted with Eq. (2) and a wrong photodetachment energy of 3.019 eV was extrapolated from the fit. Furthermore, the use of the known electron affinity as threshold energy in Eq. (2) leads to a poor agreement with the experimental data, as seen in Fig. 4. Our results seem to resolve in part this problem, since it indicates that the shape of the cross section in this energy range does not follow the Wigner law for s-wave detachment because it is largely dominated by p-wave emission. Finally, we have found a very narrow Feshbach resonance in Σ symmetry at about 3.1-eV photoelectron energy, but we did not resolve it in the total cross section since its impact is negligible (see Ref. [10] for a detailed study of C_2H^- continuum states).

B. Photodetachment of C_4H^-

The photodetachment of C_4H^- has also been extensively studied by experiments [9,15,18]. The electronic ground state of C_4H^- has $^1\Sigma^+$ symmetry with molecular orbitals $(\ldots 1\pi^4 2\pi^4 9\sigma^2)$. Through photodetachment, respectively, from the 9σ or 2π orbital, the $\widetilde{X}\,^2\Sigma^+$ or $\widetilde{A}\,^2\Pi$ state of C_4H can be formed. The two states are nearly degenerate, with an energy difference in the range of ~10–500 cm^{-1} according to various experimental and *ab initio* studies [18,34,39–42]. The best estimate is about 169 cm^{-1} and was obtained from laser-induced fluorescence spectroscopy [42]. The electron affinity (3.558 ± 0.015 eV) was measured through photoelectron spectroscopy [18].

The calculations were carried out using a similar approach as described in Sec. III A. Here, we choose a CAS of 16 MOs by including the degenerate 3π and 10σ orbitals into the reference space. The vertical excitation energy from the $\widetilde{X}\,^2\Sigma^+$ to the $\widetilde{A}\,^2\Pi$ states was calculated to be 550 cm^{-1} at the equilibrium geometry of the anion, and the vertical affinity about 3 eV. The calculated dipole moment of C_4H electronic ground state is about 0.8 D, whereas the dipole moment of the $\widetilde{A}\,^2\Pi$ state is extremely large ~5.0 D. These values are in good agreement with results obtained in other studies [34,39,43]. Although rotation of the molecule effectively reduces the dipole interaction in the long-range region, the excited valence state of C_4H has a dipole moment sufficiently large to bind an electron. Indeed, Pachkov and co-workers [44] studied the rotational structure in the origin band in the $^1A' \leftarrow X^1\Sigma^+$ electronic transition in C_4H^- and detected a dipole bound excited state with a binding energy of 240 cm^{-1} ± 100 cm^{-1} relative to its $\widetilde{A}\,^2\Pi$ parent state. Because of the unusually large dipole moment of the neutral excited state, the l and $l+1$ angular momentum channels of the detached electron are efficiently coupled in the asymptotic region up to large l values. For this reason, partial waves up to $l = 9$ had to be included in the complex Kohn calculations.

The energy dependence of the square of the transition dipole moments associated with different partial waves are plotted separately for both channels in Fig. 5. In the figure, we present individual partial wave contributions for $l \leqslant 2$ in both σ and π symmetries in order to exhibit the main features of the photodetachment process. First, one observes that s-wave emission from the lowest channel dominates for photoelectron energy lower than 0.3 eV, then p-wave emission dominates for energy below 2 eV, and finally d-wave emission becomes dominant at larger energies. From the second channel, p-wave emission largely dominates on a wide energy range.

Another interesting characteristic, already briefly discussed in the case of C_2H^-, is the behavior of the cross section just above the $\widetilde{A}\,^2\Pi$ detachment threshold. The partial cross section for s-wave photodetachment to the $\widetilde{A}\,^2\Pi$ channel is plotted in Fig. 6 as a function of the electron energy relative to the excited channel threshold energy. One observes oscillations whose widths and positions scale exponentially at lower energies, as predicted by the threshold law for l-wave

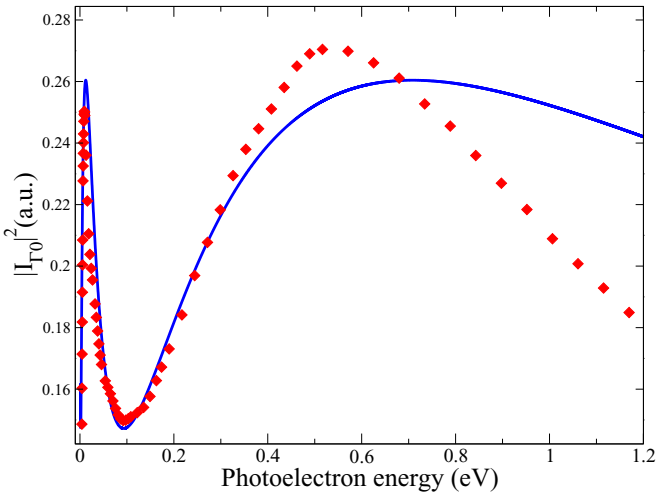

FIG. 6. (Color online) Near $\widetilde{A}\,^2\Pi$ detachment threshold values of the s-wave transition dipole moment of C_4H^- calculated with the complex Kohn variational method (diamonds) compared with the photodetachment threshold law accounting for the dipole interaction (solid line).

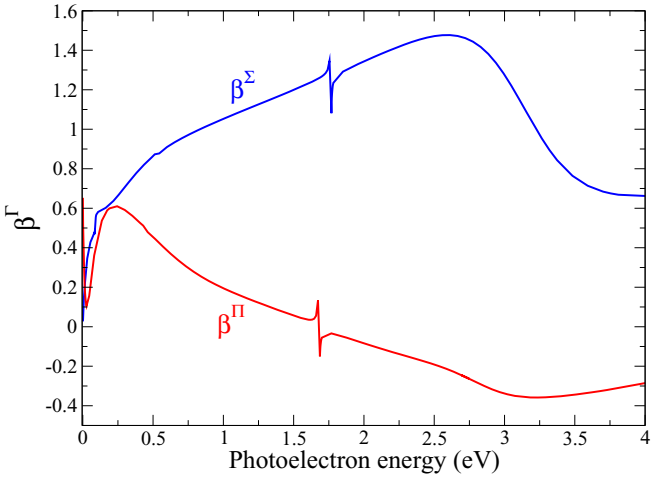

FIG. 7. (Color online) Asymmetry parameters β^Σ and β^Π for C_4H^- photodetachment as a function of the photoelectron energy relative to each channel threshold.

photodetachment [21] in the presence of a $-d/2r^2$ asymptotic potential. For $d > (l+1/2)^2$, the near-threshold cross section takes the following form:

$$\sigma_l \propto [\sinh^2(\nu\pi/2) + \cos^2(\nu \log k + \delta)]^{-1}. \qquad (14)$$

In the above equation $\nu = \sqrt{d-(l+1/2)^2}$, k is the electron wave number and δ is a short-range parameter. The above equation corresponds to the single channel case, whereas we are dealing with a multichannel problem. Nevertheless, the value of ν can be approximately determined in our case by diagonalizing the asymptotic coupled channel equations for the s- and $p\sigma$-wave emissions, which dominate at low energy. For the long-range attractive decoupled channel, we find $\nu \approx 1.55$ a.u. and the short-range parameter δ is chosen to give the best visual fit with the partial cross section obtained from the complex Kohn variational method. The near-threshold cross section obtained from Eq. (14) is presented as well in Fig. 6 and shows a good level of agreement with the Kohn calculations for electron energy below 0.5 eV. Note that the feature in the figure corresponds to the small feature seen near the $^2\Pi$ channel threshold in the lower panel of Fig. 5. Finally, there exists, in principle, an infinite number of oscillations as the electron energy decreases towards the $\widetilde{A}\,^2\Pi$ channel threshold energy. However, these oscillations cannot be observed in practice, either because their period of oscillation becomes exponentially small near threshold, or at larger energy, because their period of oscillation exceeds the rotational spacing.

We return to the discussion of Fig. 5, focusing at present on the resonance structure apparent from the value of the transition dipole moments. There exists a narrow Feshbach resonance in overall Π symmetry located at about 5.3-eV photon energy, which results in a spike in the value of the transition dipole moments. At about 6-eV photon energy appears a mixed p- and d-wave Π shape resonance associated with the lowest $^2\Sigma$ channel. Furthermore, let us mention that we have also found a broad d-wave shape resonance in overall Σ symmetry associated with the second channel and centered at about 9-eV photon energy.

The calculated values of the asymmetry parameters for both channels are presented in Fig. 7. As in the case of C_2H^- photodetachment, direct comparison to experimental data is complicated by several factors that are not accounted for in our FC approach. However, our results seem to follow the trend observed in [18] for photodetachment spectra recorded at 4.657 eV (1.1-eV photoelectron energy), namely $\beta > 0$ for peaks corresponding to detachment from the $\widetilde{X}\,^2\Sigma^+$ channel and $\beta \cong 0$ for peaks corresponding to detachment from the $\widetilde{A}\,^2\Pi$ channel. Quantitatively, asymmetry parameters to the lowest $\widetilde{X}\,^2\Sigma^+$ channel were measured to be 0.29 for the ground-state peak, 0.62 and 0.81 for two vibrationally excited peaks, while we obtained $\beta^\Sigma = 1.07$ at 1.1-eV photoelectron energy. For photodetachment to the $\widetilde{A}\,^2\Pi$ channel, Taylor *et al.* [18] measured asymmetry parameters to be 0.00, -0.01, and -0.37 for different vibrationally excited peaks while we obtained $\beta^\Pi = 0.15$. Note that the estimated average errors is ± 0.25 in the measured asymmetry parameters given in Ref. [18].

The Franck-Condon factors are calculated using Eq. (13) derived from the harmonic approximation. Equilibrium positions and vibrational frequencies were obtained with similar *ab initio* methods than presented in Sec. III A for the case of C_2H^- photodetachment. We have again found that the vibrational frequencies and normal coordinates are similar for the different electronic states, thus confirming the validity of the approximations used to derive Eq. (13). Our results were then compared with values reported in Refs. [41,44]. Of course, for such a large hydrocarbon chain, the various molecular characteristics depend, to a certain extent, on the type of calculation performed. Nevertheless, an overall reasonable agreement was obtained, such that our calculated FC factors should represent a fairly good estimation and should not induce a significant error in the total cross section. We obtained $|\langle\zeta^-_{v_o}|\zeta^\Sigma_{v_o}\rangle|^2 = 0.75$ and $|\langle\zeta^-_{v_o}|\zeta^\Pi_{v_o}\rangle|^2 = 0.88$ for the values of the FC factors.

The total cross section is plotted in Fig. 8 as a function of the photon energy and compared with two experimental

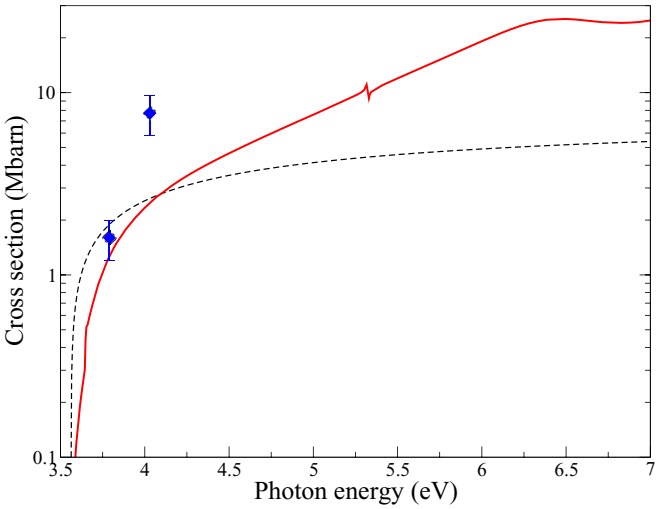

FIG. 8. (Color online) Total cross section (solid line) in C_4H^- photodetachment as a function of the photon energy. The dashed line represents the model defined in Eq. (2) with the known electron affinity as threshold energy and taking $\sigma_\infty = 7.7$ Mbarn determined in Ref. [9]. Experimental points are taken from Ref. [9] with associated 25% error bars.

values measured close to the photodetachment threshold [9]. The agreement is good for the lowest energy point, at 3.79-eV photon energy, whereas the experimental value at 4.03-eV photon energy is more than a factor two larger than the result obtained from our calculations. The same discrepancy was actually observed by Best and co-workers [9] while fitting their results using Eq. (2) and is also plotted in the figure. One possible explanation could be that the latter energy point is situated on the top of a vibrational Feshbach resonance. In fact, a progression of such resonances was observed in the low-energy photodetachment of C_4H^- by Pinot *et al.* [15] and appear as a large increase of the cross section. Finally, the effects of the different resonances described above is clearly reflected on the total cross section.

C. Photodetachment of C_6H^-

The experimental study of the photodetachment of C_6H^- was also conducted by Best *et al.* [9] and Pinot *et al.* [15]. Theoretical calculations of the photodetachment of C_6H^- is rendered difficult by the demanding computational work needed to describe such a large molecule. Using once more the general approach detailed in Sec. III A, we have calculated the structural characteristics of the anion ground state and of its associated radical states, and compared our results with available data in the literature.

As the number of carbon atoms of the hydrocarbon radical chains increases, it is a known fact that the energy of the lowest $^2\Pi$ state decreases more rapidly than the $^2\Sigma$ state energy. As a consequence, C_6H and the larger hydrocarbon-chain radicals have $\widetilde{X}\,^2\Pi$ ground-state symmetry. In the case of C_6H, the ground state can be formed through photodetachment from the HOMO of the $\widetilde{X}\,^1\Sigma$ anion ground state, which has the main electronic configuration $(\ldots 2\pi^4 13\sigma^2 3\pi^4)$. The first excited $\widetilde{A}\,^2\Sigma$ state of C_6H is formed by photodetachment from the 13σ MO and lies 0.21 eV above C_6H ground-state energy according to our calculations. This value compares well with the measurement (0.181 eV) of Taylor *et al.* [18], and lies between the values calculated by Woon [34] (0.11 eV) and Sobolewski [45] (0.25 eV). The second excited state $\widetilde{B}\,^2\Pi$, formed through photodetachment of an electron from the 2π orbital of C_6H^-, lies only 2.3 eV above the C_6H ground state according to precise spectral measurements by Zhao and co-workers [46]. Because we are mainly interested in the low-energy part of the photodetachment cross section, where experimental data are available, our calculation is optimized to describe at best the lowest radical states and the anion ground state. It is the reason why our excitation energy to the second excited state of C_6H is largely overestimated ($\sim$1 eV). Thus, our calculations do not include the effect of this channel as it opens at photoelectron energies above 2.3 eV. Note that the second excited states of the smaller hydrocarbons have larger excitation energies and our cross sections should include the effect of all open channels in the energy range considered. Finally, we have obtained permanent dipole moments of 5.6 and 0.8 D for the $\widetilde{X}\,^2\Pi$ and $\widetilde{A}\,^2\Sigma$ states of C_6H, respectively. These values are in good agreement with past *ab initio* calculations reported in Refs. [47,48].

Because of the extremely large dipole moment of C_6H in its $\widetilde{X}\,^2\Pi$ electronic ground state, the C_6H^- anion should support dipole bound states. Indeed, Pinot *et al.* [15] found a large band in their spectrum corresponding to a bound-bound transition of C_6H^- anion. Actually, Engelking [49] showed that for polar molecules possessing a symmetry axis containing a nonzero component of angular momentum (e.g., for a linear molecule with projection of electronic angular momentum different from zero), the asymptotic dipole moment does not average to zero. For a molecule with a permanent dipole moment μ, total angular momentum J, and projection K along the symmetry axis, neglecting K doubling, inversion splitting, and assuming a $\Delta J = 0$ coupling scheme, Engelking derived that the reduced dipole moment takes the simple form $\mu_{\rm av} = \mu K/\sqrt{J(J+1)}$. As a consequence, it is expected that C_6H^- possesses, if not an infinity, at least several excited dipole states. Moreover, as already discussed at length in Sec. III B, the threshold behavior in the photodetachment cross section of C_6H^- is expected to be different than the usual Wigner threshold law [see Eq. (14)]. Indeed, our calculations clearly demonstrate that several low-energy partial wave transition dipole moments, shown in Fig. 9, oscillate as a function of the electron energy. However, as noted before, the extremely small rotational constants of the large hydrocarbon chains would hinder the experimental observation of these oscillations.

We note from Fig. 9 that the d-wave transition dipole moments rapidly dominate other partial waves with increasing photon energy, whereas p-wave emission was dominant on a wide energy range in the case of C_2H^- and C_4H^- photodetachment. As a consequence, the asymmetry parameters presented in Fig. 10 are not as large as in the previous cases. On the other hand, we have found a resonance structure similar to C_4H^-; a low energy Feshbach resonance in Π symmetry at 4.3-eV photon energy and a mixed p- and d-wave Π shape resonance associated mainly with the $^2\Sigma$ channel and centered at about 6.2-eV photon energy. Evidence of this resonance is particularly well demonstrated in the β^Σ asymmetry parameter

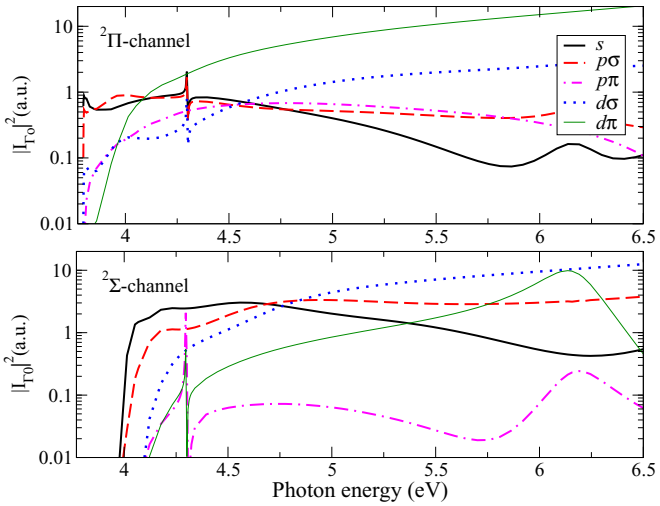

FIG. 9. (Color online) Square of the transition dipole moments of C_6H^- for different partial waves associated with the $^2\Pi$ (upper panel) and $^2\Sigma^+$ (lower panel) channels as a function of the photon energy.

in Fig. 10. Our calculated values of the asymmetry parameters at 4.657-eV photon energy are $\beta^{\Pi} = 0.60$ and $\beta^{\Sigma} = -0.05$, whereas Taylor *et al.* [18] measured $\beta^{\Pi} = 0.22 \pm 0.25$ and $\beta^{\Sigma} = 0.48 \pm 0.25$.

Precise equilibrium geometries for the anion electronic ground state and neutral ground and first excited electronic states are difficult to obtain in the case of C_6H^-. For instance, the CCSD method, which was used for the smaller hydrocarbon chains is computationally extremely demanding for this molecule. To the best of our knowledge, no high level *ab initio* calculations of the equilibrium geometries of all the different states are available in the literature. On the other hand, determination of the stable geometries for these states have been performed at the Hartree-Fock (HF) level in [47,50]. Actually, HF calculations are expected to give relatively

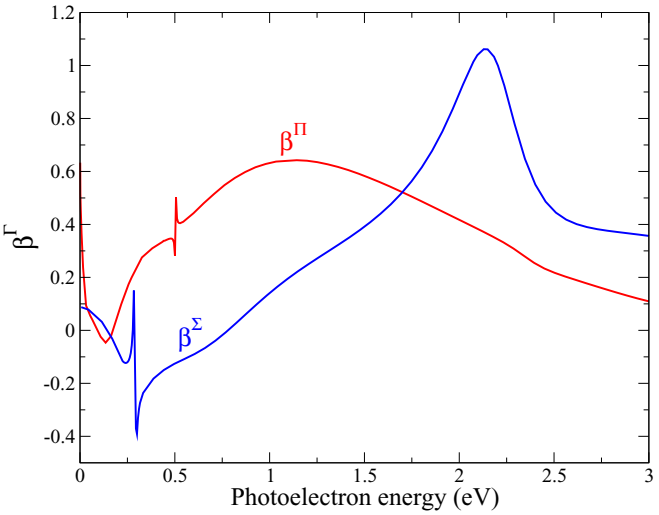

FIG. 10. (Color online) Asymmetry parameters β^{Σ} and β^{Π} for C_6H^- photodetachment as a function of the photoelectron energy relative to each channel threshold.

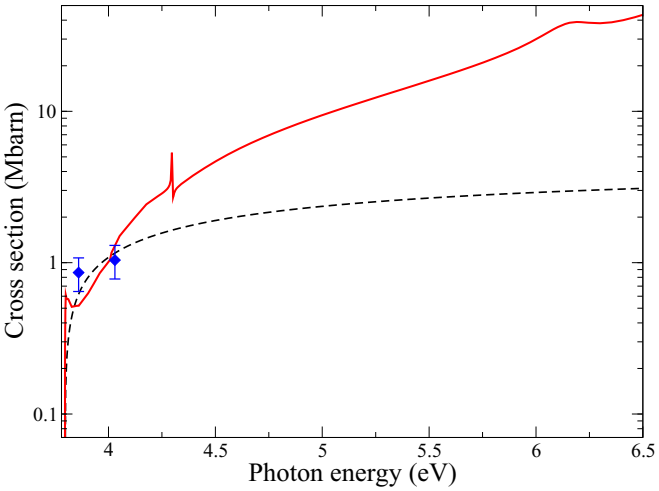

FIG. 11. (Color online) Total cross section (solid line) in C_6H^- photodetachment as a function of the photon energy. The dashed line represents the model defined in Eq. (2) with the known electron affinity as threshold energy and taking $\sigma_\infty = 4.8$ Mbarn determined in Ref. [9]. Experimental points are taken from Ref. [9] with associated 25% error bars.

good estimations of equilibrium positions, at least, accurate enough for the purpose of this study on photodetachment. Therefore, we have performed our calculations at the HF level and the results agree well with the values reported in Refs. [47,50]. We also computed the vibrational frequencies and normal coordinates needed in Eq. (13). Finally, we obtained $|\langle\zeta^-_{v_o}|\zeta^{\Pi}_{v_o}\rangle|^2 = 0.86$ and $|\langle\zeta^-_{v_o}|\zeta^{\Sigma}_{v_o}\rangle|^2 = 0.78$ for the values of the FC factors.

The theoretical cross section is plotted in Fig. 11 as a function of the photon energy. Also shown in the figure, the two experimental points measured by Best and co-workers [9] and the fit from Eq. (2) with the known electron affinity as threshold energy. Our calculation agrees rather well with the experimental results at both energy points. Nevertheless, the computed value at 3.86 eV underestimates the experimental cross section by about 30%. This discrepancy is most likely due to the unphysical large oscillation in our cross section near threshold, which originates from the neglect of the rotational motion. These oscillations are indeed not apparent from the low-energy photodetachment spectrum of Pinot and co-workers [15]. Also, note that the opening of the second channel is responsible for a quick rise of the cross section above 4.01 eV. Finally, the effect of the shape resonance is barely noticeable from the total cross section.

IV. CONCLUSION

We have presented a theoretical study of the photodetachment of the C_2H^-, C_4H^-, and C_6H^- anions using the complex Kohn variational method and the Franck-Condon approximation. Our results are compared with recent experimental data on absolute photodetachment cross sections [9]. An overall good agreement is observed for the three hydrocarbon-chain anions apart from a large discrepancy at one-photon energy for C_4H^-. In particular, we have considered the threshold behavior of the cross sections, the effects of excited channels,

and electronic resonances. The results indicate that the model of Millar and co-workers [16] is not always able to describe the photodetachment near the lowest threshold because p-wave emission might rapidly dominate the cross section for some anions. Furthermore, our calculations demonstrate that open excited radical channels can lead to a significant rise of the cross section above the channel threshold energies. In addition, we have also computed values of the asymmetry parameters, which give information about the angular distribution in the photodetachment of each anion and compare them with different experimental measurements [15,18,19]. Some of the hydrocarbon radical states have a large permanent dipole moment, which significantly modifies the usual Wigner threshold law for the cross section. We have verified that the complex Kohn method reproduces the correct threshold law derived by O'Malley [21]. The modified threshold law leads to oscillations of the cross section with a logarithmically increasing period. These oscillations are not observable in practice because of rotational effects, which are neglected in our treatment. Moreover, our approach does not include vibrational and nonlocal effects, such that our cross sections lack the vibrational structure present in the experimental spectra. Vibrational Feshbach resonances are not present in our photodetachment cross sections and may produce important effects. For instance, it is possible that the discrepancy with the experimental result in C_4H^- photodetachment at 4.03-eV photon energy could potentially be explained by the presence of such a resonance around that energy. Treating these effects to explain the experimental spectra is a challenging task, which could be the subject of future studies.

ACKNOWLEDGMENTS

This work is supported by the US Department of Energy Office of Basic Energy Science and the National Science Foundation (NSF), Grants No. PHY-11-60611 and No. PHY-10-68785. A.E.O. acknowledges support from the National Science Foundation, with some of this material based on work while serving at NSF.

[1] M. C. McCarthy, C. A. Gottlieb, H. Gupta, and P. Thaddeus, Astrophys. J. Lett. **652**, L141 (2006).
[2] J. Cernicharo, M. Guelin, M. Agundez, K. Kawaguchi, and P. Thaddeus, A&A **467**, L37 (2007).
[3] H. Gupta, S. Brünken, F. Tamassia, C. A. Gottlieb, M. C. McCarthy, and P. Thaddeus, Astrophys. J. Lett. **655**, L57 (2007).
[4] K. Kawaguchi, R. Fujimori, S. Aimi, S. Takano, E. Y. Okabayashi, H. Gupta, S. Brünken, C. A. Gottlieb, M. C. McCarthy, and P. Thaddeus, Publ. Astron. Soc. Jpn. **59**, L47 (2007).
[5] P. Thaddeus, C. A. Gottlieb, H. Gupta, S. Brunken, M. C. McCarthy, M. Agundez, M. Guelin, and J. Cernicharo, Astrophys. J. **677**, 1132 (2008).
[6] J. Cernicharo, M. Guélin, M. Agúndez, M. C. McCarthy, and P. Thaddeus, Astrophys. J. Lett. **688**, L83 (2008).
[7] M. Agúndez, J. Cernicharo, M. Guélin, C. Kahane, E. Roueff, J. Klos, F. J. Aoiz, F. Lique, N. Marcelino, J. R. Goicoechea, M. González García, C. A. Gottlieb, M. C. McCarthy, and P. Thaddeus, A&A **517**, L2 (2010).
[8] E. Herbst, Nature (London) **289**, 656 (1981).
[9] T. Best, R. Otto, S. Trippel, P. Hlavanka, A. von Zastrow, S. Eisenbach, S. Jézouin, R. Wester, E. Vigren, M. Hamberg, and W. D. Geppert, Astrophys. J. **742**, 63 (2011).
[10] S. Harrison and J. Tennyson, J. Phys. B: At. Mol. Opt. Phys. **44**, 045206 (2011).
[11] S. Harrison and J. Tennyson, J. Phys. B: At. Mol. Opt. Phys. **45**, 035204 (2012).
[12] S. S. Kumar, D. Hauser, R. Jindra, T. Best, Š. Roučka, W. D. Geppert, T. J. Millar, and R. Wester, Astrophys. J. **776**, 25 (2013).
[13] N. Douguet, S. Fonseca dos Santos, M. Raoult, O. Dulieu, A. E. Orel, and V. Kokoouline, Phys. Rev. A **88**, 052710 (2013).
[14] F. Carelli, M. Satta, T. Grassi, and F. A. Gianturco, Astrophys. J. **774**, 97 (2013).
[15] T. Pinot, M. Tulej, F. Güthe, M. Pachkov, and J. P. Maier, J. Chem. Phys. **116**, 6126 (2002).
[16] T. J. Millar, C. Walsh, M. A. Cordiner, R. N. Chuimín, and E. Herbst, Astrophys. J. Lett. **662**, L87 (2007).
[17] K. M. Ervin and W. C. Lineberger, J. Phys. Chem. **95**, 1167 (1991).
[18] T. R. Taylor, C. Xu, and D. M. Neumark, J. Chem. Phys. **108**, 10018 (1998).
[19] J. Zhou, E. Garand, and D. M. Neumark, J. Chem. Phys. **127**, 114313 (2007).
[20] E. P. Wigner, Phys. Rev. **73**, 1002 (1948).
[21] T. F. O'Malley, Phys. Rev. **137**, A1668 (1965).
[22] K. J. Reed, A. H. Zimmerman, H. C. Andersen, and J. I. Brauman, J. Chem. Phys. **64**, 1368 (1976).
[23] A. E. Orel and T. N. Rescigno, Phys. Rev. A **41**, 1695 (1990).
[24] D. L. Lynch and B. I. Schneider, Phys. Rev. A **45**, 4494 (1992).
[25] T. N. Rescigno, B. H. Lengsfield III, and A. E. Orel, J. Chem. Phys. **99**, 5097 (1993).
[26] S. Miyabe, D. J. Haxton, K. V. Lawler, A. E. Orel, C. W. McCurdy, and T. N. Rescigno, Phys. Rev. A **83**, 043401 (2011).
[27] T. N. Rescigno, B. H. Lengsfield III, and C. W. McCurdy, *Modern Electronic Structure Theory 1* (World Scientific, Singapore, 1995).
[28] T. N. Rescigno, C. W. McCurdy, A. E. Orel, and B. H. Lengsfield III, *Computational Method for Electron-Molecule Collisions* (Plenum Press, New York, 1995).
[29] C. W. McCurdy and T. N. Rescigno, Phys. Rev. A **39**, 4487 (1989).
[30] C. S. Trevisan, A. E. Orel, and T. N. Rescigno, Phys. Rev. A **68**, 062707 (2003).
[31] A. E. Orel, T. N. Rescigno, and B. H. Lengsfield, Phys. Rev. A **44**, 4328 (1991).
[32] C. S. Trevisan, C. W. McCurdy, and T. N. Rescigno, J. Phys. B: At. Mol. Opt. Phys. **45**, 194002 (2012).

[33] T. N. Rescigno, N. Douguet, and A. E. Orel, J. Phys. B: At. Mol. Opt. Phys. **45**, 194001 (2012).
[34] D. E. Woon, Chem. Phys. Lett. **244**, 45 (1995).
[35] M. Peric, R. J. Buenker, and S. D. Peyerimhoff, Mol. Phys. **71**, 673 (1990).
[36] Q. Cui and K. Morokuma, J. Chem. Phys. **108**, 626 (1998).
[37] D. Duflot, J.-M. Robbe, and J.-P. Flament, J. Chem. Phys. **100**, 1236 (1994).
[38] M. Bogey, C. Demuynck, and J.-L. Destombes, Mol. Phys. **66**, 955 (1989).
[39] M. C. McCarthy, C. A. Gottlieb, P. Thaddeus, M. Horn, and P. Botschwina, J. Chem. Phys. **103**, 7820 (1995).
[40] J. Zhou, E. Garand, and D. M. Neumark, J. Chem. Phys. **127**, 154320 (2007).
[41] M. L. Senent and M. Hochlaf, Astrophys. J. **708**, 1452 (2010).
[42] K. Hoshina, H. Kohguchi, Y. Ohshima, and Y. Endo, J. Chem. Phys. **108**, 3465 (1998).
[43] S. Graf, J. Geiss, and S. Leutwyler, J. Chem. Phys. **114**, 4542 (2001).
[44] M. Pachkov, T. Pinot, M. Tulej, F. Güthe, K. Tikhomirov, and J. P. Maier, Mol. Phys. **101**, 583 (2002).
[45] A. L. Sobolewski and L. Adamovicz, J. Chem. Phys. **102**, 394 (1995).
[46] D. Zhao, M. A. Haddad, H. Linnartz, and W. Ubachs, J. Chem. Phys. **135**, 044307 (2011).
[47] A. Murakami, K. Kawaguchi, and S. Saito, Publ. Astron. Soc. Jpn. **39**, 189 (1987).
[48] F. Pauzat and Y. Ellinger, Astron. Astrophys. **216**, 305 (1989).
[49] P. C. Engelking, Phys. Rev. A **26**, 740 (1982).
[50] R. Liu, X. Zhou, and P. Pulay, J. Chem. Phys. **97**, 1602 (1992).